Radiation Effects & Defects in Solids
Vol. 167, No. 9, September 2012, 651–658

Energetic electron emission from a ferroelectric sample during incomplete surface discharge

V.Tz. Gurovich[a], V. Raikhlin[a], G. Bazalitski[a], J. Felsteiner[a], Ya.E. Krasik[a]* and I. Haber[b]

[a]*Physics Department, Technion, Haifa 32000, Israel;* [b]*IREAP, University of Maryland, College Park, MD 20742, USA*

(*Received 10 October 2011; final version received 7 January 2012*)

In this paper, the results of simplified analytical modeling and particle-in-cell numerical simulations of plasma formation and propagation along the surface of a ferroelectric sample under the application of a negative driving pulse to the rear solid electrode are presented. These models allow one to reproduce the main characteristics of the incomplete discharge. In particular, it is shown that the experimentally observed energetic electrons are related to the secondary emission electron acceleration in the sheath between the plasma and the ferroelectric surface. Also, simulation results show that secondary electron emission significantly decreases the surface plasma density while increasing its propagation velocity and that high desorption rate of the neutrals is required to sustain surface plasma formation.

Keywords: plasma; ferroelectric; surface discharge; electron beam

PACS: 52.50Dg; 84.70.+p; 52.25.Tx

1. Introduction

The phenomenon of copious energetic electron emission from different ferroelectric samples (FS) covered by strip-like front and solid rear electrodes (see Figure 1) induced by the application of a pulse of several kilovolts was intensively studied during the last two decades (*1*, *2*).

It was shown that this energetic electron emission occurs without the application of voltage for electron extraction from the FS. A specific feature of this electron emission is its occurrence primarily during the nanosecond time scale rise and fall times of the driving pulse $\varphi_{dr}(t)$ with electron current density up to several tens of A cm^{-2}. The time-dependent electron energy, E_e, was found to qualitatively follow the negative driving pulse applied to the rear electrode and the energy of electrons emitted at the edge of the strip was less than half the energy of electrons emitted in the middle between the strips (*3*). When a negative driving pulse was applied to the front electrode, no difference was observed for electrons emitted at the edge of the strip and in the middle between the strips and the energy of the electrons followed $e\varphi_{dr}(t)$. With the positive driving pulse, high-energy electrons were only obtained early in the driving pulse. It has been

*Corresponding author. Email: fnkrasik@physics.technion.ac.il

ISSN 1042-0150 print/ISSN 1029-4953 online

http://dx.doi.org/10.1080/10420150.2012.656640
http://www.tandfonline.com

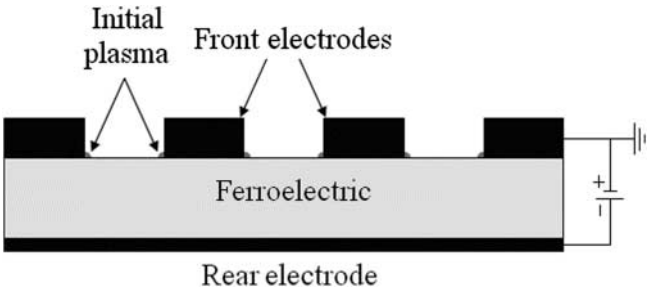

Figure 1. Schematic view of the ferroelectric plasma source.

suggested that this energetic electron emission occurs from the plasma formed in the FS by incomplete surface discharges initiated at triple points (*4*) at the edges of the front electrode. The electron temperature T_e and density n_e of the surface plasma were found to be in the range 2–8 eV and 10^{17}–10^{21} m^{-3}, respectively (*2*, *5*, *6*). Such plasma can be considered as a low-resistive one so that the potential of the plasma is almost equal to that of the front electrode. Thus, one can assume that this plasma is a source of energetic electrons. This assumption is correct only when a negative driving pulse is applied to the front electrode. Indeed, when a positive driving pulse is applied to either the rear or the front electrodes, the plasma potential is either zero or positive with respect to the grounded electrode, which does not allow electron emission from the plasma and is in agreement with the electron energy measurement (*3*). However, intense electron emission was obtained when a negative driving pulse was applied to the rear electrode when the front electrode was grounded and the plasma could not be considered as the source of energetic electrons.

In this paper, we present a simplified analytical model and results of two-dimensional particle-in-cell (2D PIC) simulations explaining the formation of an energetic electron beam during the application of a negative driving pulse to the rear electrode. It is shown that in this case, the generation of energetic electrons occurs due to intense secondary electron emission (SEE) from the FS front surface induced by plasma ions interacting with the FS surface.

2. Analytical model

Let us consider a simplified model of an FS (a dielectric constant $\varepsilon >> 1$) covered by a solid rear electrode and a grounded strip-like front electrode. The application of a negative driving pulse to the rear electrode leads to the formation of a plasma layer (PL) propagating along the FS front surface. This PL serves as a dynamic front electrode of the capacitor formed by the FS with the rear solid electrode having capacitance per unit surface $C_0 = \varepsilon\varepsilon_0/h$, where h is the FS thickness. For simplicity, an FS with unit width and a PL propagating with a constant velocity U are considered. The potential difference between the electrodes is $\phi_0 = \text{const}$ and the potential of the PL is equal to that of the front electrode. Between the FS and the PL, an ion electrical layer (IEL) with a constant potential difference φ_0 exists. From the PL boundary toward the FS, a constant ion saturation current density, $J_i = 0.5eN_iV_S$, is emitted, where N_i is the density of the ions in the PL bulk, $V_S = (k_BT_e/m_i)^{1/2}$ is the ion sound velocity, k_B is the Boltzmann constant and m_i is the ion mass. The plasma ions which interact with the FS surface supply to the PL desorbed neutrals by ionizing the plasma electrons and becoming the source of the PL. Assuming that for stationary IEL, the values of N_i and T_e are constant, the plasma front velocity component perpendicular to the PL boundary is $V_n = V_S = \text{const}$. In Cartesian coordinates with the *OX*- and the *OY*-axis directed along and perpendicular to the FS surface, respectively, the evolution of the

PL boundary can be defined by a function $y(t,x)$ satisfying Equation (7):

$$\frac{\partial y}{\partial t} = -\frac{V_S}{\sqrt{1+(\partial y/\partial x)^2}}. \tag{1}$$

The rate of increase of the FS surface positive charge density $\sigma(t,x)$ is

$$\frac{\partial \sigma}{\partial t} = 0.5eV_S N_i A|\varphi|^\beta \cos\alpha(t,x). \tag{2}$$

Here, the value of $\cos\alpha(t,x)$ is determined by the inclination of the PL boundary to the FS surface at the point x. The effect of SEE is accounted by the term $A|\varphi|^\beta >> 1$, where A is the coefficient. This term determines the yield of SEs formed by one interacting ion. The value $\beta > 0$ corresponds to an increase in the yield of SEs with the increase in the energy of ions interacting with the FS. The positive charge density distribution along the FS surface and potential difference in the IEL govern the dynamics of the PL boundary determined by

$$\frac{y(t,x)}{y_0} = \left[\frac{\varphi(t,x)}{\varphi_0}\right]^{3/4}. \tag{3}$$

Here, y_0 and φ_0 are the IEL thickness and the potential difference between the FS and the PL front, respectively, and $y(t,x)$ and $\varphi(t,x)$ are their current values. The FS surface positive charge density reads

$$\sigma(x,t) = C_0|\varphi_0|(1-\psi), \tag{4}$$

where $\psi = \varphi(t,x)/\varphi_0$ is the normalized potential. Equation (4) accounts for the polarization non-compensated negative charge which appears at the FS surface as a result of the application of a negative driving pulse. Equation (2) solution is considered in the form of a wave with argument $\xi = x - Ut$:

$$\frac{l_* d\psi}{d\xi} = \psi^\beta \cos\alpha(t,x). \tag{5}$$

Here, $l_* = C_0|\varphi_0|U/0.5BeV_S N_i$ is a typical charging length of the FS and the dimensionless parameter $B = A|\phi_0|^\beta$determines the number of SEs with energy $e\phi_0$. Equations (1) and (3) can be rewritten using the dimensionless coordinate $\varsigma = \xi/l_*$ and the thickness of the IEL $z = y/l_*$ as the equation for the potential distribution along the FS surface:

$$\frac{Mz_0 \mathrm{d}(\psi^{3/4})}{\mathrm{d}\varsigma} = \frac{1}{\sqrt{1+(\mathrm{d}z/\mathrm{d}\varsigma)^2}}. \tag{6}$$

Here, $M = U/V_S$ and $z_0 = y_0/l_*$. Now, using Equation (5) and considering that $\mathrm{d}z/\mathrm{d}\varsigma = \mathrm{tg}\alpha(\varsigma)$, one obtains the equation for the same potential distribution, when $\beta = 1/4$:

$$\frac{(4/3)d(\psi^{3/4})}{d\varsigma}/ = \frac{1}{\sqrt{1+(\mathrm{d}z/\mathrm{d}\varsigma)^2}}. \tag{7}$$

The identity of Equations (6) and (7) determines that $z_0 = 4/(3M)$. The solution of Equations (6) and (7), which gives the potential distribution along the FS surface, reads

$$\psi(\varsigma) = \frac{\varphi(\varsigma)}{\varphi_0} = \left[1 + \frac{3}{4}MF(M)(\varsigma - 1)\right]^{4/3}. \tag{8}$$

Here, $F(M) = [(\sqrt{M^2+4} - M)/(2M)]^{1/2}$. Now, using Equations (3) and (8) and the dimensionless parameters, one obtains the equation for the PL boundary as

$$z(\varsigma) = z_0 + (\varsigma - 1)F(M). \tag{9}$$

At the front of the PL ($\varsigma = \xi/l_* = 1$), the thickness of the IEL equals $z_0 = 4/(3M)$, and it decreases linearly toward the strip electrode ($\varsigma < 1$).

The model also predicts the energy distribution for the SEs accelerated by the IEL potential. Indeed, using Equation (2) and assuming that the typical charging time of the FS capacitor is$\tau \approx L/U$, where L is the typical length of the FS capacitor, one obtains

$$n_{se}(E_e) = 0.5e^{-1/4}V_S N_i A E_e^{1/4} \cos\alpha(t,x) L U^{-1}. \tag{10}$$

Now, let us compare the results of the model with the experimental results presented in (*2*, *5*, *6*), where $T_e \approx 5 \pm 2\,\text{eV}$ and $N_i \approx 10^{19}\,\text{m}^{-3}$ were determined. If the main sources of the plasma are the hydrogen atoms desorbed from the surface, in this case, $V_S \approx 2.2 \times 10^4\,\text{m/s}$. Also, the experimental data show that during $\Delta t \approx 50\,\text{ns}$ of the driving pulse, the plasma propagates along the distance $L \approx 0.5\,\text{cm}$ that results in $U \approx 10^5\,\text{m s}^{-1}$, $M \approx 4.5$ and the inclination angle $\alpha = \text{arctg}[F(M)] \approx 12^0$ of the PL boundary. Also, experimental data show that during $\Delta t \approx 50\,\text{ns}$, the PL charges an FS capacitor with an area of $\sim 1\,\text{cm}^2$ up to $\phi_0 \approx 4\,\text{kV}$ (*3*). The latter allows one to estimate charging current density $j \approx 50\,\text{A cm}^{-2}$ for $C_0 = 0.13\,\text{nF}$ ($\varepsilon = 1000$ and $h = 4 \times 10^{-3}\,\text{m}$) that results in $B \approx 10$.

3. Numerical model

A detailed description of the 2D PIC simulations (*8*) carried out using the WARP (*9*) software will be published elsewhere. The physical model considers a 4-mm thick sample and either 10 or 100 or 1000 dielectric constant of the FS placed between the grounded front strip-like electrodes with a distance of 3 mm between the strips and the rear electrode (Figure 1) supplied by a negative voltage pulse having a sine form. The initial plasma (in the simulations, a hydrogen plasma was considered) is generated at the triple point at $\varphi = 1\,\text{kV}$ (*4*), since subsequent evolution of the plasma was found to be almost independent of the details of this initial plasma excitation. Simulations are started at $\varphi = 1\,\text{kV}$ with a quarter of period (rise time) τ_r of either 10 or 20 ns and φ_{dr} of either 4 or 8 kV with the initial plasma having dimensions $50\,\mu\text{m} \times 50\,\mu\text{m}$, density $n_e = 10^{22}\,\text{m}^{-3}$ and $T_e = 8\,\text{eV}$. An ion impinging on the FS surface desorbs the neutrals and the secondary electrons (SEs) (zero initial energy) with yield functions $Y_n = Y_n(E_i)$ and $Y_e = Y_e(E_i)$. For an ion with energy E_i, a desorbed neutral has the energy $E_n = E_i/Y_n$ on average. In the simulation runs, different yield functions were tested (*8*) so as to sustain plasma formation and not to produce too many neutrals. Neutrals are assumed to have Maxwellian distribution with a spread of $0.5\sqrt{E_n}$ in velocities. When neutrals enter the plasma, they are ionized by the plasma electrons with the probability of ionizing being $p = <\sigma_{ion} V_e > n_e \mathrm{d}t$, where $\sigma_{ion} \approx 10^{-21}\,\text{m}^2$ is the ionization cross section, V_e is the velocity of electrons, n_e is the electron density and $\mathrm{d}t$ is the period of time over which the probability is calculated. In the simulations, an adjustable time step was used with $\omega_p dt \leq 1.5$, where ω_p is the plasma frequency and $V_e \mathrm{d}t/\mathrm{d}x \leq 0.5$, where $\mathrm{d}x$ is the mesh resolution.

First, the simulations showed that self-consistent plasma formation and propagation along the FS surface occur only for $n_e \geq 10^{20}\,\text{m}^{-3}$ and $Y_n \approx 10$. Such a high value of Y_n can be expected in the case of high-energy ($\geq$100 eV) plasma ions interacting with a dielectric surface (*10*) and suggest that sputtering processes and adsorbed gas layers govern the plasma formation. The latter

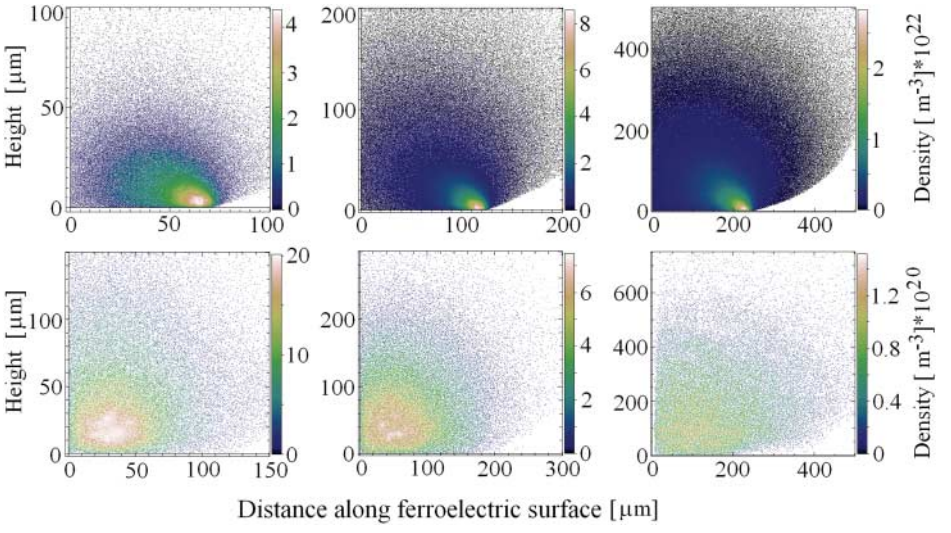

Figure 2. Evolution of plasma density: (a) without SEE and (b) with SEE. $\varphi_{dr} = 4\,\text{kV}$, $\tau_r = 10\,\text{ns}$.

is in agreement with the spectroscopic data showing the presence of desorbed gases and bulk material in the surface plasma (*5*). The evolution of the plasma density is shown in Figure 2 for the FS with $\varepsilon = 100$ and $\varphi_{dr} = 4\,\text{kV}$ with $\tau_r = 10\,\text{ns}$. Similar results were obtained for the cases of driving pulses with $\varphi_{dr} = 4\,\text{kV}$, $\tau_r = 20\,\text{ns}$ and $\varphi_{dr} = 8\,\text{kV}$, $\tau_r = 10\,\text{ns}$. One can see that when SEE is included, the average value of n_e decreases and the largest plasma density is obtained close to the strip electrode and not at its front as in the case without SEE. The decreased plasma density in the case of SEE is explained by the faster charging of the FS. The value of n_e obtained with SEE is in agreement with the data obtained in earlier experimental studies (*5*). Also, the simulations showed that the values of n_e and U decrease when φ_{dr} reaches its maximal amplitude and do not change in time. The latter is also in agreement with the experimental data showing plasma formation mainly during the rise and fall times of the driving pulse (*11*).

The potential distributions along the FS surface at different times with and without SEE for the FS with $\varepsilon = 100$ and $\varphi_{dr} = 4\,\text{kV}$, $\tau_r = 10\,\text{ns}$ are shown in Figure 3. One can see that in the case

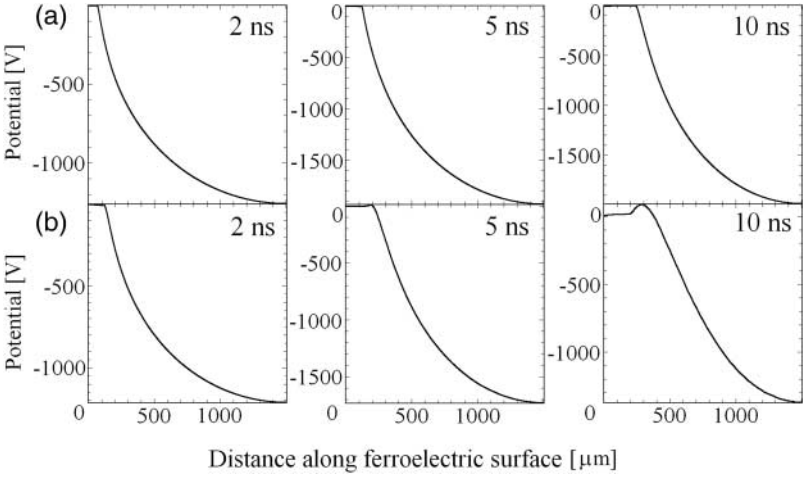

Figure 3. Potential distribution along the FS at different times of the driving pulse: (a) without SEE and (b) with SEE. $\varphi_{dr} = 4\,\text{kV}$, $\tau_r = 10\,\text{ns}$.

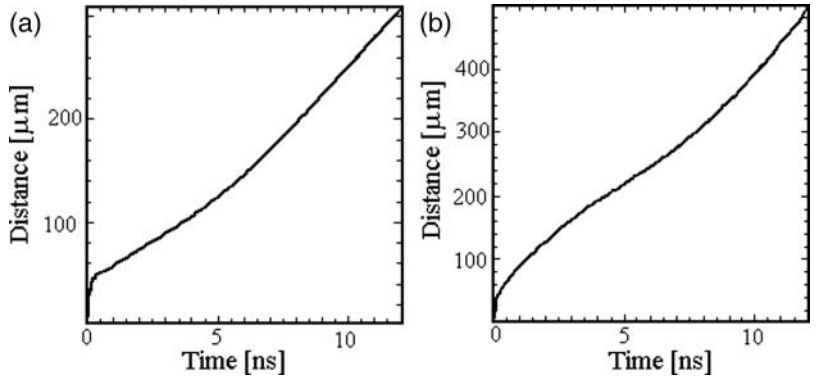

Figure 4. Evolution of the PL front: (a) without SEE and (b) with SEE. $\varphi_{dr} = 4\,\text{kV}$, $\tau_r = 10\,\text{ns}$.

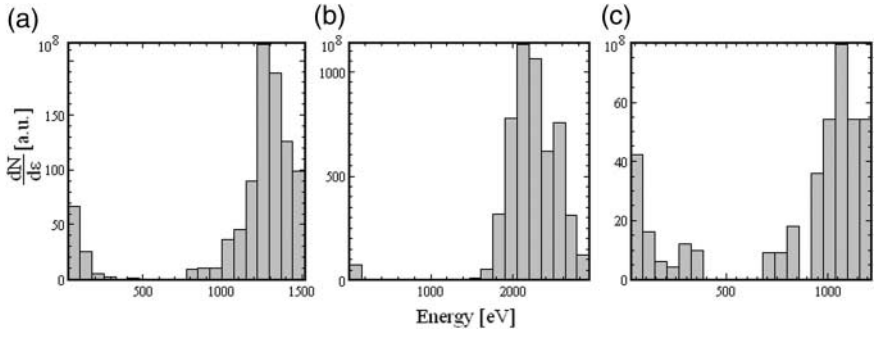

Figure 5. Energy spectra of SEs: (a) $\varphi_{dr} = 4\,\text{kV}$, $\tau_r = 10\,\text{ns}$; (b) $\varphi_{dr} = 8\,\text{kV}$, $\tau_r = 10\,\text{ns}$; and (c) $\varphi_{dr} = 4\,\text{kV}$, $\tau_r = 20\,\text{ns}$.

of SEE, in front of the plasma [a location with a potential of $(2-3)T_e$], the FS surface potential is significantly smaller than that when SEE is absent due to a decrease in the surface polarization charge by SEs in addition to the plasma ion compensation. Also, the simulations showed that the larger the amplitude or the faster the rise time of the driving pulse, the larger the difference in potential distributions between cases with and without SEE.

In Figure 4, the evolution of the plasma front propagation with and without SEE is presented for the FS with $\varepsilon = 100$ and $\varphi_{dr} = 4\,\text{kV}$, $\tau_r = 10\,\text{ns}$. One can see that SEE increases the value of U almost twofold. A similar dependence is observed for the increased value of φ_{dr}. These results are consistent with the potential distribution showing a strong dependence on the SEE and φ_{dr}. The simulations for surface plasma formation for the FS with different values of ε (with and without SEE) showed a decrease in U and an increase in n_e with the increase of ε, which is in agreement with the data (*2*, *3*, *4*).

The energy spectra of SEs for different values of φ_{dr} and τ_r (see Figure 5) demonstrate that the SEs acquire significant energy. Thus, these electrons can be considered as the source of the high-energy electron beam obtained in experiments when a negative driving pulse was applied to the rear electrode and the front strip-like electrode was grounded (*2*, *3*). Also, one can see that the faster the value of τ_r, the more energetic the emitted electron beam.

The energy spectra of the SEs also depend on the location of the FS surface where these electrons were emitted. Namely, the energy spectrum of the SEs emitted from the surface close to the strip consists of low-energy electrons (see Figure 6). Oppositely, in the case of SEs emitted from the surface in the middle between the strips, one obtains an energy spectrum with high-energy electrons. These results are in agreement with the experimental results (*3*) showing that most of the energetic electrons are emitted from the location in the middle between the strips.

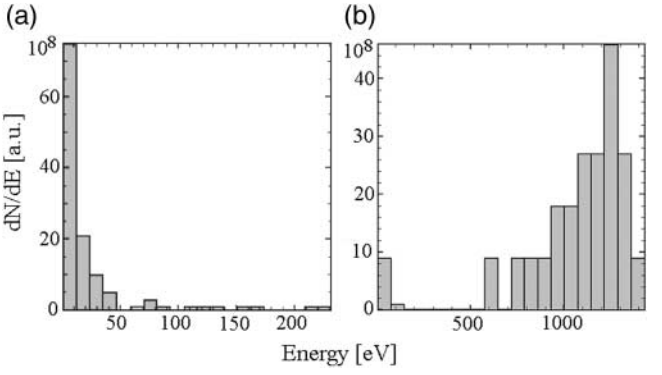

Figure 6. Energy spectra of the SEs emitted from the FS at distances (a) 0–0.75 mm and (b) 0.75–1.5 mm with respect to the strip electrode. $\varphi_{dr} = 4\,kV$, $\tau_r = 10\,ns$.

4. Summary

The developed analytical model allows one to reproduce the main parameters of the incomplete discharge (n_e, U and $\varphi(t,x)$) along the FS. Also, the model explains the experimentally obtained energetic electron beam generation by the SEs emitted from the FS and accelerated by the surface potential. The 2D PIC simulations of the PL formation and propagation along the FS, which consider surface charging, neutral desorption, ionization processes and SEE, indicate the following main features:

- The evolution of the surface plasma along the FS occurs only at $n_e \geq 10^{20}\,m^{-3}$ and $Y_n \approx 10$. These data suggest that sputtering processes and adsorbed gas layers govern the plasma formation, which is in agreement with the spectroscopic measurements (*5*).
- The simulations show that plasma formation considerably weakens when the applied voltage reaches its maximum and does not change in time. The latter is in agreement with the experimental data showing plasma formation during the rise in the driving pulse (*11*).
- It has been shown that an increase in ε leads to a decrease in the plasma propagation velocity, which is consistent with the experimental data (*2*, *11*).
- The simulations show that the surface plasma formation is accompanied by the generation of a high-energy electron beam. This beam consists of SEs induced by the interaction of the plasma ions with the FS and accelerated by the FS front surface potential. These results are in agreement with the experimental data (*3*). SEE also increases the rate of the ferroelectric charging, which results in the surface plasma formation with increased U and n_e.

Acknowledgements

We thank Igor Kaganovich for fruitful discussions and D.P. Grote for his significant assistance with the simulation code. This research was supported by the US-Israel Binational Science Foundation, Grant No. 2006373.

References

(1) Riege, H.; Boscolo, I.; Handerbek, J.; Herleb, U. *J. Appl. Phys.* **1998,** *84,* 1602–1617.
(2) Rosenman, G.; Shur, D.; Krasik, Ya.E.; Dunaevsky, A. *J. Appl. Phys.* **2000,** *88,* 6109–6161.
(3) Dunaevsky, A.; Krasik, Ya.E.; Felsteiner, J.; Krokhmal, A. *J. Appl. Phys.* **2000,** *87,* 3270–3278.
(4) Mesyats, G.A. *Explosive Electron Emission* (in Russian); URO: Ekaterinburg, 1998.
(5) Dunaevsky, A.; Chirko, K.; Krasik, Ya.E.; Felsteiner, J.; Bernshtam, V. *J. Appl. Phys.* **2001,** *90,* 4108–4114.
(6) Chirko, K.; Krasik, Ya.E.; Felsteiner, J.; Sternlieb, A. *J. Appl. Phys.* **2002,** *92,* 5691–5697.

(7) Whitham, G.B. *Linear and Nonlinear Waves*; Wiley: New York, 1974.
(8) Raikhlin, V. *Ferrolectric Plasma Source Modeling Using the Particle-in-Cell Method*; M.Sc. Thesis, Technion: Haifa, Israel, 2010.
(9) Vay, J.L.; Colella, P.; Kwan, J.W.; McCorquodale, P.; Serafini, D.B.; Friedman, A.; Grote, D.P.; Westenskow, G.; Adam, J.C.; Heron, A.; Haber, I. *Phys. Plasma* **2004,** *11,* 2928–2934.
(10) Behrisch, R., Ed. *Sputtering by Particle Bombardment*; Springer: Berlin, 1981.
(11) Dunaevsky, A.; Krasik, Ya.E.; Felsteiner, J.; Dorfman, S. *J. Appl. Phys.* **1999,** *85,* 8464–8473.